Exciton Dynamics in a One-Dimensional Self-Assembling Lyotropic Discotic Liquid Crystal

Rhian E. Hughes, Simon P. Hart, and D. Alastair Smith*

Department of Physics and Astronomy and Astbury Centre for Structural Molecular Biology, University of Leeds, Leeds, U.K. LS2 9JT

Bijan Movaghar, Richard J. Bushby, and Neville Boden

Centre for Self-Organising Molecular Systems, University of Leeds, Leeds, U.K. LS2 9JT

Received: November 1, 2001; In Final Form: February 27, 2002

The steady state and time resolved phophysical properties of a novel self-assembling lyotropic discotic liquid crystal, 2,3,6,7,10,11-hexa-(1,4,7-trioxaoctyl)-triphenylene (TP6EO2M) are reported. The spectral changes that accompany the formation of linear aggregates in D_2O provide no evidence of excited-state delocalization, and the evidence suggests only a very weak interaction between neighboring molecules. Time resolved fluorescence depolarization measurements support a picture of a mobile exciton that hops along the columnar aggregates at a rate of at least 10^{11} s^{-1}. Since the system comprises an isotropic solution of columnar aggregates, the exciton motion is likely to be highly one dimensional. Doping of the molecular aggregates introduces extrinsic trap sites allowing a simple 1-D hopping model to be used to analyze the long time fluorescence decay kinetics. Fitting the data obtained from samples doped with trinitrofluorononone indicates that this lyotropic system has an order of magnitude higher concentration of intrinsic traps in the isotropic phase than its thermotropic analogues display in the columnar mesophase.

Introduction

Energy and charge transfer in (quasi) one-dimensional systems have received a great deal of attention in the past two decades for both fundamental and technological reasons, and systems that display *truly* one-dimensional transport properties will be of great importance in future molecular electronic and photonic devices.[1−4] The organic materials that have been investigated in most detail in this context include conjugated polymers and molecular aggregates[5−12] and thermotropic liquid crystals.[13−16] The extensive work of Markovitsi and co-workers[17−22] on the electronic energy transfer mechanisms in triphenylene-based thermotropic liquid crystals has revealed that, although the systems possess anisotropic phase structure, the singlet exciton dynamics display a dimensionality greater than unity (note that triplet excitons in these systems display 1-D transport[23]). These self-organizing thermotropic discogens only allow the properties of the chromophore to be studied in the liquid crystalline state in which the columns are separated by only ca. 2 nm. Self-assembling lyotropic discotic liquid crystals give isotropic and columnar nematic phases in which the linear molecular aggregates in solution are effectively isolated from each other and which should show truly one-dimensional exciton dynamics.[24−30] Molecular self-assembly therefore presents interesting and unique systems with strong analogies to biological energy transport structures in which to extend current studies of energy transport in molecular materials.

The triphenylene-based lyotropic mesogen 2,3,6,7,10,11-hexa-(1,4,7-trioxaoctyl) triphenylene (TP6EO2M) has been designed to self-assemble into columnar aggregates and self-organize into columnar mesophases in aqueous solution [24,25] (see Figure 1).

One-dimensional linear self-assembly is a thermodynamically driven process, the extent of which is dependent upon concentration, pressure, and temperature, and a polydisperse distribution of aggregate sizes will be present under any given set of conditions. The relationship between concentration and average aggregate length has been investigated for dilute solutions of TP6EO2M using proton NMR,[26] and extensive studies of the self-assembly and self-organization of the aqueous system have been reported.[26,31−38] Properties such as aggregate flexibility and persistence length have been found to influence the liquid crystalline behavior, and the distribution of aggregate lengths is well described both by a model which considers the

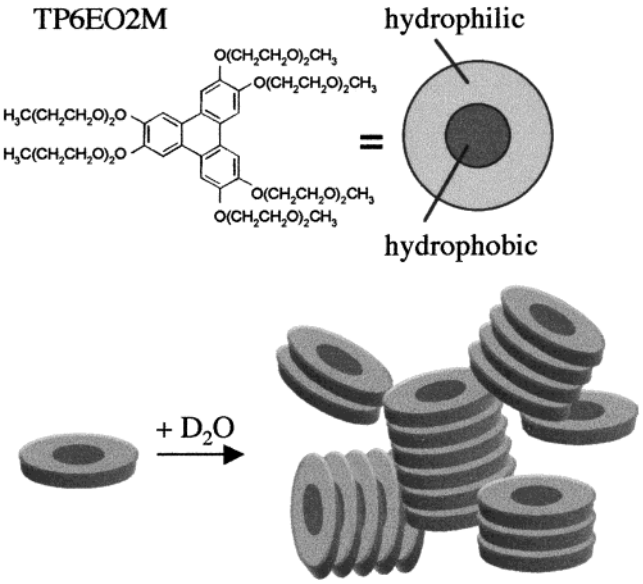

Figure 1. Structure of the lyotropic discotic liquid crystal, 2,3,6,7,10,11-hexa-(1,4,7,10-trioxaoctyl)-triphenylene (TP6EO2M) and schematic representation of the self-assembly process into linear aggregates in aqueous solution.

* Corresponding author. E-mail: damsmith@leeds.ac.uk. Tel +44 113 233 3875. Fax +44 113 233 3900.

10.1021/jp014028o CCC: $22.00
Published on Web 06/12/2002

concentration dependence of the free energy of monomer contact and by the lattice gas model.[39,40] Indeed, the TP6EO2M/water system is probably the most completely understood example of one-dimensional self-assembly.

Hence, the TP6EO2M/water system in the isotropic phase presents a valuable opportunity to study the photophysical properties of a truly one-dimensional system, whose average aggregation number (i.e., length of the aggregates) can be varied with concentration in a precisely controlled manner. The monomer concentration and solution temperature also permit controlled entry in to a variety of liquid crystalline phases that might be assumed to have higher dimensionality of energy transport analogous to the observations in thermotropic discotic systems. This then, is a versatile molecular material in which to study single- and multidimensional energy (or charge) transport.

A preliminary characterization of the photophysical properties of the TP6EO2M monomer using UV−visible absorption, steady state fluorescence, and Raman and time resolved fluorescence spectroscopy has been reported.[41] In this paper we present a detailed study of the effect of linear self-assembly on the energy transport along these isolated aggregates in the isotropic lyotropic phase. We report on steady state and time resolved fluorescence intensity and depolarization measurements in the presence and absence of extrinsic traps introduced into the aggregates in the form of a molecular dopant, trinitrofluorononе (TNF). We propose a description of the excited state dynamics in which a localized but mobile exciton undergoes one-dimensional migration along the aggregates until it encounters a trap or an end which results in rapid nonradiative decay.

Experimental Section

TP6EO2M was synthesized as described previously.[24,25] The solvents D_2O and HPLC grade DCM were purchased from Fluorochem (Glossop, UK) and EM Industries (Gibbstown, NJ), respectively. Samples of varying concentration were prepared by successive dilution of a concentrated stock solution. Nitrogen was bubbled through the solvent prior to solution preparation to minimize dynamic quenching of fluorescence by triplet oxygen. UV-vis absorption spectra were obtained using a Perkin-Elmer Lambda 2 spectrophotometer (Beaconsfield, UK) and steady state luminescence spectra were obtained using a Perkin-Elmer LS50−B fluorimeter.

Fluorescence lifetime measurements were made using the time correlated single photon counting technique with front face sample geometry. (Front face geometry was used because at high TP6EO2M concentrations the optical density of the samples was too high to use 90 degrees geometry with a bulk solution). The second harmonic (532 nm) of a mode locked Nd:YAG laser (Coherent Antares) running at 76 MHz was used to synchronously pump a dye laser (Coherent, 700 series) circulating Rhodamine 6G. The cavity dumped dye laser output (562 nm at 4 MHz) was then frequency doubled using BBO to give the required excitation wavelength of 281 nm. Fluorescence decays were obtained using an Edinburgh Instruments FL900-CDT spectrometer (Livingstone, UK) with a Hamamatsu R3809 microchannel plate PMT (Welwyn Garden City, UK), providing an instrument function fwhm of approximately 70 ps. The time resolved decay data were fitted by iterative reconvolution with an assumed decay law using the measured instrument function. The quality of the least-squares fitting procedure was evaluated by the reduced χ^2 values, the residuals and the autocorrelation of the residuals using the commercial software (Edinburgh Instruments). Anisotropy measurements were made with vertically polarized excitation at 365 nm. The emission polarizer alternated between vertical and horizontal until 1000 counts were collected in the peak of both fluorescence decays. The G factor was measured using a solution of aniline with horizontally polarized light.

Trinitrofluorononе (TNF) was chosen as an extrinsic dopant for exciton trapping studies since from previous work in which thermotropic phases of TP6EO2M/TNF mixtures were characterized[42,43] it is known to intercalate between TP6EO2M molecules. Exciton trapping studies in this lyotropic system require that the dopant remains within the aggregates in aqueous solution and that a random distribution of dopant molecules is achieved. To achieve this the following doping procedure was used. HPLC tetrahydrafuran (THF) and TNF were obtained from Aldrich (Gillingham, UK). The TNF was used as received, but the THF was freshly distilled for each experiment. The THF/TNF/TP6EO2M solution (with the TNF:TP6EO2M doping ratio as required) was placed on a watch glass until the majority of the solvent had evaporated and the remaining solvent was removed under vacuum over a period of 48 h. Doped TP6EO2M was then made up in D_2O immediately prior to use.

Results and Discussion

Effects of Self-Assembly and the Exciton Hopping Model. Figure 2a,b shows the absorption spectra of TP6EO2M as a function of concentration in DCM and D_2O, respectively. The form of the absorption curve of TP6EO2M in DCM is almost identical to that of HAT6 (the thermotropic discotic analogue) in solution,[44] with virtually no dependence on concentration within the range studied here. Detailed CSINDO calculations[19,21] for the triphenylene-based chromophore have led to the following assignments of the absorption peaks. The lowest energy absorption peaks at 345 and 359 nm, most clearly observed in D_2O, are attributed to the S_0-S_1 transition, and the shoulder at 330 nm is attributed to the S_0-S_2 transition, both of which are symmetry forbidden but weakly allowed by vibronic coupling. The two main absorption peaks at 307 and 277 nm correspond to the S_0-S_3 and S_0-S_4 transitions, respectively. The peaks/shoulders at 269, 260, and 251 nm form part of a vibronic series with an energy spacing that corresponds to the energy of one of the main peaks in the Raman spectrum excited at 632 nm in D_2O.[45]

At these concentrations in D_2O, self-assembly leads to an isotropic distribution of columnar aggregates with a length distribution that increases with increasing concentration. For example, at 10^{-6} M in D_2O at 298 K the weight average aggregation number is 1−2 and at 5×10^{-3} M it is ∼15. At the highest concentrations used here, $\sim 10^{-1}$ M, the average aggregate length is of the order 25 monomers, but these are of course average values and the solution will contain a distribution of aggregate sizes about the mean. Self-assembly or aggregation does not occur in DCM at these concentrations, and therefore TP6EO2M exists in monomeric form in this solvent.

The absorption spectrum at the lowest concentration in D_2O is very similar to those across the range of concentrations in DCM. There is a slight blue shift and a general decrease in extinction coefficient by a factor of about 2 in D_2O. The effects of self-assembly in D_2O as concentration increases are quite marked. The total oscillator strength of each electronic transition is relatively unaffected, but there is a clear shift in the distribution between the vibronic transitions of S_0-S_4. These quite significant changes in vibrational overlap are not reflected by changes in the Raman spectra of solutions of TP6EO2M in D_2O (data not shown), suggesting that the ground state

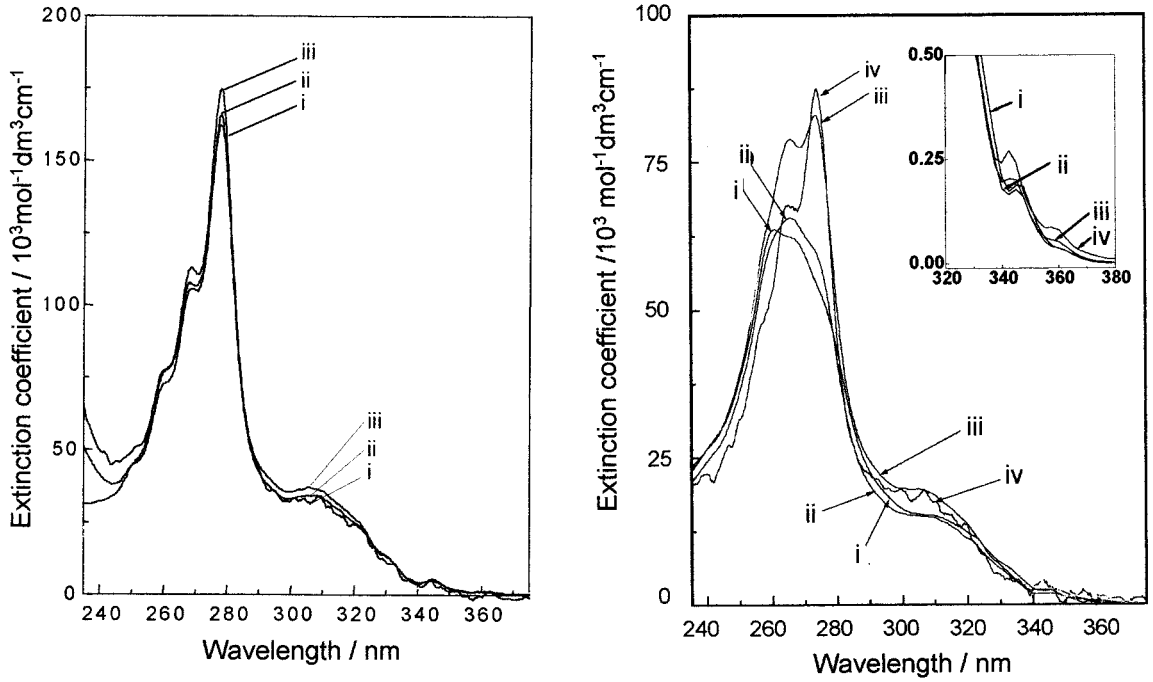

Figure 2. Absorption spectra of TP6EO2M in (a) DCM: (i) 10^{-4} M, (ii) 10^{-5} M, and (iii) 10^{-6} M) and (b) D_2O: (i) 10^{-3} M, (ii) 10^{-4} M, (iii) 10^{-5} M, (iv) 10^{-6} M). Inset in (b) shows a $\times 10$ magnification of the red edge absorption features in D_2O.

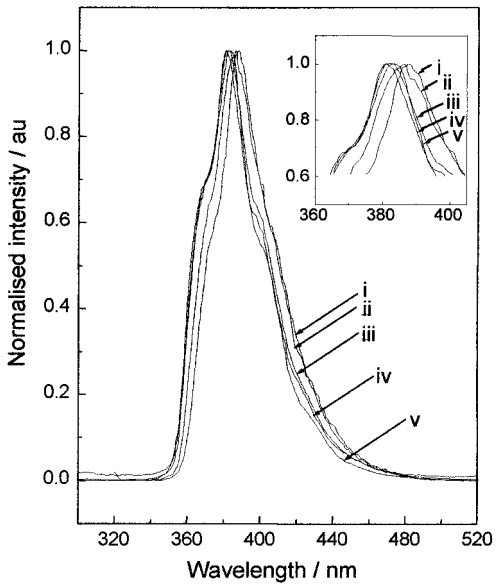

Figure 3. Normalized fluorescence emission spectra of TP6EO2M excited at 280 nm in D_2O: (i) 10^{-3} M, (ii) 10^{-4} M, (iii) 10^{-5} M, (iv) 10^{-6} M, and in DCM (v) 10^{-6} M. Inset expands the region around the emission peak to highlight the small red shift with increasing concentration.

chromophores are only interacting weakly within the aggregates. Therefore, one concludes that self-assembly affects the excited state geometry leading to the observed changes in the absorption spectra.

Figure 3 shows the steady state fluorescence emission spectra of TP6EO2M as a function of concentration in D_2O and of a dilute (10^{-6} M) solution in DCM for comparison. The emission peak in D_2O shifts to lower energy with increasing concentration, with a total shift of 474 cm^{-1} (0.058 eV) over this concentration range. This shift corresponds to approximately 2 kT, indicating that there is no significant excited state delocalization (red shifts of 0.2−1 eV are observed, for example, in conjugated polymers[46]). In fact, the small red shift of the emission peak may simply be due to a skewing of the spectrum caused by the change in the strength of neighboring vibronic contributions noted in the absorption spectrum, or possibly due to reabsorption. The absorption and emission spectra therefore indicate that there is very little $\pi-\pi$ interaction between neighboring triphenylene cores within the aggregates, which is consistent with the relatively large disc−disc separation of 4.5 Å.[26,31]

TABLE 1: Results of Fitting a Single Exponential Function with Decay Constant, τ_f, to the Long Time (>5 ns) Fluorescence Decays of TP6EO2M as a Function of Concentration in D_2O and at a Single Concentration in DCM[a]

conc. TP6EO2M (M)	solvent	τ_f (ns)	χ^2
10^{-1}	D_2O	18.5 ± 0.7	0.92
5×10^{-2}	D_2O	18.7 ± 0.7	1.10
10^{-2}	D_2O	18.2 ± 0.7	1.02
5×10^{-3}	D_2O	18.2 ± 0.7	1.16
10^{-3}	D_2O	16.9 ± 0.6	1.08
10^{-4}	D_2O	16.0 ± 0.6	1.01
10^{-5}	D_2O	14.3 ± 0.5	1.06
10^{-6}	D_2O	12.8 ± 0.5	1.06
10^{-6}	DCM	8.3 ± 0.3	1.08

[a] In all cases excitation wavelength was 280 nm and emission wavelength was 389 nm. Quality of fit is indicated by the χ^2 value and evaluated by inspection of the residuals.

Three examples of the time-resolved fluorescence decays of TP6EO2M in D_2O and DCM at an excitation wavelength of 281 nm and an emission wavelength of 389 nm are shown in Figure 4 along with the residuals of fits to single-exponential decays. The results of fitting the decays after the peak with a single-exponential decay are summarized in Table 1. In DCM the decay was fitted well by a single-exponential model with a lifetime of 8.3 ± 0.3 ns independent of concentration, reflecting the monomeric state of TP6EO2M in this solvent across this range of concentrations. The decays in D_2O could be adequately fitted using a single-exponential function in each case, but the quality of fit declined at short times as concentration was

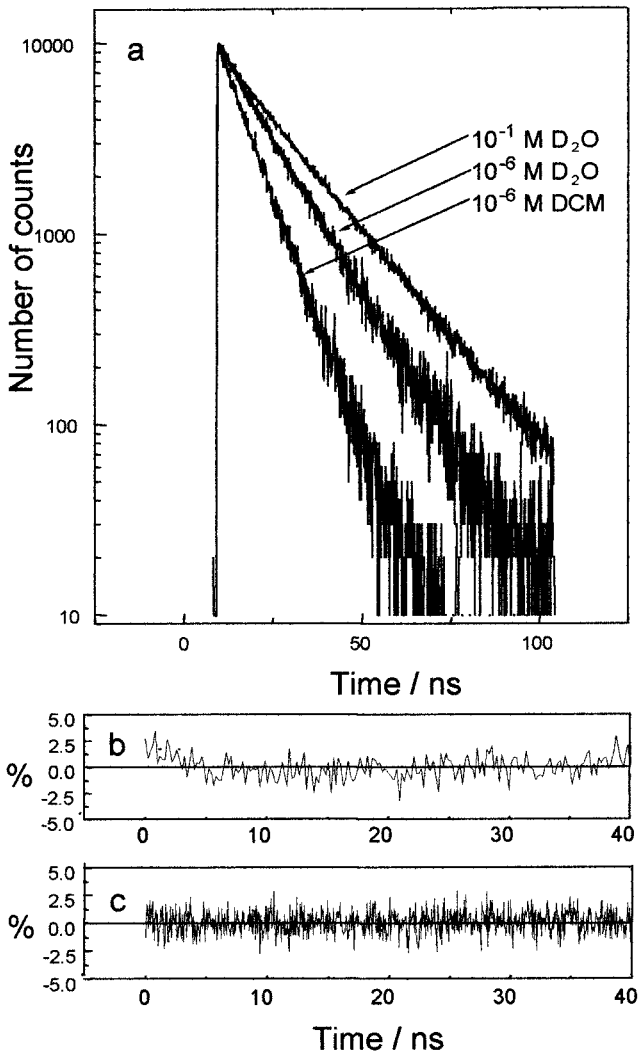

Figure 4. (a) Time resolved fluorescence decays and fits to single-exponential functions of TP6EO2M: (a) 10^{-1} M and 10^{-6} M in D_2O; 10^{-6} M in DCM. Excitation wavelength was 280 nm and emission wavelength was 389 nm in all cases. Residuals to single-exponential fits to the data for (b) 10^{-1} M in D_2O and (c) 10^{-6} M in D_2O.

increased, as can be seen by the residuals for the highest and lowest concentration samples in Figure 4. At the higher concentration, although the χ^2 value (Table 1) is good, the residuals indicate that the fit at short times is not adequate and this decay was fitted better using a distribution of exponential lifetimes (Gaussian distribution of 50 lifetimes) with a mean value of 18.3 ns and standard deviation of 4 ns. The results of fitting the fluorescence decays in D_2O therefore indicate a strong dependence on aggregation. The fluorescence lifetime increases from a monoexponential decay of 12.8 ± 0.5 ns at 10^{-6} M to a distribution with mean value of 18.3 ns at 10^{-1} M, reflecting the distribution in aggregation number at this concentration. At the lowest concentration in D_2O (10^{-6} M), at which concentration the solution comprises mainly monomers and dimers, the fitting yields a decay constant that is considerably slower than that of the monomer in DCM, which could be due to the difference in dielectric constant of the solvent or to the reduction in nonradiative rate within small aggregates in the size distribution.

To test this, a range of different solvents was used to investigate the effect of dielectric constant on the photophysical properties of TP6EO2M at a concentration of 10^{-6} M. The solvents used provided a range of dielectric constants from 70 to 9 (D_2O: $\epsilon = 70$, acetonitrile: $\epsilon = 40$, methanol: $\epsilon = 32$, ethanol: $\epsilon = 24$, propanol: $\epsilon = 20$ and DCM: $\epsilon = 9$). The absorption and steady state luminescence spectra showed virtually no dependence on dielectric constant (data not shown) apart from the reduction in extinction coefficient in D_2O already commented upon. Table 2 summarizes the effect on the time resolved fluorescence decays of the solvent dielectric constant. An effect is observed in D_2O compared with the other solvents, but there is no dependence on dielectric constant, suggesting that the increase in fluorescence lifetime observed in D_2O is due to the range of aggregate sizes even at this low average aggregation number.

TABLE 2: Effect of the Solvent Dielectric Constant, ϵ, on the Fluorescence Lifetime, τ_f, for 10^{-6} M Solutions of TP6EO2M[a]

solvent	ϵ	τ_f (ns)	χ^2
D_2O	70	12.8 ± 0.5	1.06
acetonitrile	40	8.9 ± 0.3	1.24
methanol	33	9.1 ± 0.3	1.26
ethanol	24	9.3 ± 0.3	1.35
propanol	20	9.5 ± 0.3	1.21
DCM	9	8.3 ± 0.3	1.08

[a] In all cases excitation wavelength was 280 nm and emission wavelength was 389 nm. Quality of fit is indicated by the χ^2 value and evaluated by inspection of the residuals.

In earlier work we showed that the fluorescence quantum efficiency of TP6EO2M is independent of aggregate size and has a value of 0.15 for excitation at 280 nm and emission at 389 nm, which is similar to values of quantum yield reported for HAT6 in solution (0.2 [18] and 0.135 [47]). The observed increase in fluorescence lifetime with increasing aggregate size therefore suggests that the radiative rate is also increasing, reflecting a change in the excited state of TP6EO2M with aggregation. However, this would be reflected by changes in the absorption spectrum which are not observed. In fact, measurement of quantum yield is not straightforward, especially in concentrated solutions of a molecule that has a very high extinction coefficient, and any such results have a large uncertainty. The increase in fluorescence lifetime is therefore most likely to be the result of a decrease in the nonradiative rate in larger aggregates. This reduction in nonradiative rate due to aggregation saturates around 5×10^{-3} M, corresponding to an average aggregate size of $\sim$15.

A similar increase in fluorescence lifetime as a function of aggregation has been reported for other triphenylene-based alkoxy compounds where the fluorescence lifetime increased from 8.3 to 13.4 ns as concentration was increased from 10^{-7} M to 10^{-3} M.[47] This was also attributed to a "distribution of aggregate lengths", but the exact interpretation is not clear.

In systems such as TP6EO2M aggregates, a mobile exciton should result in a rapid depolarization of fluorescence emission if dipole moments of neighboring chromophores are noncollinear. The time scale of this anisotropy decay will depend on the hopping rate, which will in turn depend on the nature of the energy transport process. Flexibility of the aggregates and rotational/translational diffusion in solution will also cause a loss in fluorescence polarization which would occur on a slower time scale, especially in larger aggregates. Time-resolved fluorescence anisotropy experiments are therefore a powerful probe of molecular and exciton dynamics in this system.

Figure 5 shows the time resolved fluorescence anisotropy decays of TP6EO2M in D_2O as a function of concentration, i.e., aggregate size (curves a−e), and at the two extreme concentrations in DCM (curves f and g). These decays are not

TABLE 3: Summary of the Results of Fitting the Time Resolved Fluorescence Anisotropy Decays of TP6EO2M in D_2O (curves a−e in Figure 5) and in DCM (curves f and g in Figure 5) with a Biexponential Function with Decay Constants, τ_1 and τ_2, and Initial Anisotropy Value at $T = 0$ of r_o[a]

conc. TP6EO2M (M)	solvent	Figure 4 curve	τ_1 (ns)	α_1 %	τ_2 (ns)	α_2 %	r_0
10^{-1}	D_2O	a	2.131	100			0.015
10^{-2}	D_2O	b	1.903	25	0.170	75	0.075
10^{-3}	D_2O	c	1.412	43	0.214	57	0.095
10^{-4}	D_2O	d	1.352	66	0.121	34	0.100
10^{-5}	D_2O	e	1.032	35	0.154	65	0.170
10^{-1}	DCM	f	1.009	25	0.218	75	0.070
10^{-5}	DCM	g	1.010	10	0.180	90	0.070

[a] Quality of fit was evaluated by a χ^2 analysis and inspection of the residuals.

fitted satisfactorily by a single-exponential decay (apart from the case of 10^{-1} M in D_2O), and the results of fitting with a biexponential function are summarized in Table 3. The anisotropy decays in D_2O show a strong dependence on aggregation. At the highest concentration in D_2O there is an almost complete and instantaneous initial loss in anisotropy to an r_o value of 0.015, which is faster than our instrument resolution (~100 ps). There is a subsequent monoexponential decay in anisotropy with a time constant of approximately 2.1 ns. As concentration is decreased and the weight average aggregation number decreases, the r_o value increases reflecting a smaller initial loss in anisotropy and the subsequent decays become distinctly biexponential. If the anisotropy decay was due solely to the rotational/translational diffusion of the aggregates in solution, then as average aggregate size increased the observed anisotropy decay would become slower. The long time decay does indeed become slower, increasing from 1 to 2 ns at the highest concentration, but the anisotropy decays to zero almost instantaneously, which is commensurate with the migration of an exciton along the aggregates. The anisotropy results provide an indication of the order of magnitude of the exciton hopping rate in the aggregates. Since there is an almost complete loss in anisotropy within the instrument response (~100 ps), it is reasonable to infer that the hopping rate is at least 10^{11} s^{-1} and possibly faster, which is in agreement with the results obtained for doped samples of the thermotropic analogue HAT6 (~10^{12} s^{-1}).[22,23]

In DCM and at low concentration in D_2O the anisotropy decays are commensurate with monomers or very short aggregates rotating freely in solution. The shorter, predominant decay constant, τ_2, remains roughly constant in DCM and throughout the concentration range in D_2O, suggesting that it describes the rotational diffusion around the long axis of the aggregates. The value is comparable to the rotational correlation time of related monomeric systems (e.g., P5−17, a derivative of perylene with long flexible alkyl chains, which has a rotational correlation time of 0.220 ns[48] in 2-methyltetrahydrofuran. The flexible chains have a considerable effect on the rotational motion of the monomer as is the case for P5−17 for which the rotational correlation time of the perylene core is 0.038 ns [49] in the same solvent). The longer time constant therefore presumably describes the end-over-end tumbling of the aggregates and thus increases as weight average aggregation number increases.

We propose the following simple model. A localized but mobile excited state migrates along the aggregates until it relaxes to the ground state either at an intrinsic trap site or at a site where the nonradiative rate is high such as the ends of the aggregates that are partially exposed to solvent. In long aggregates there is an almost complete loss in anisotropy on a time scale too fast to measure with our apparatus due to this exciton migration, suggesting a hopping rate of at least 10^{11} s^{-1}. A slow and measurable depolarization of the fluorescence emission caused by rotational diffusion of the aggregates in solution is also observed.

Luminescence Studies in the Presence of Extrinsic Traps. A straightforward method of determining the hopping rate that has been employed with the thermotropic analogues is to use extrinsic traps which are introduced into the aggregates as dopant molecules. Subsequently, a 1-D hopping model which incorporates the trap concentration can be used to fit the fluorescence decay kinetics.

Trinitrofluorononone (TNF) has previously been shown to intercalate within the columnar aggregates of TP6EO2M, and its photophysical properties make it ideal as an extrinsic trap in this system, i.e., its absorption spectrum overlaps the emission spectrum of the host chromophore and it is not itself fluorescent.

Figure 6 shows the effect on the time-resolved fluorescence decays of 10^{-2} M TP6EO2M solutions in D_2O doped with a range of concentrations of TNF. As TNF concentration is increased the fluorescence decay becomes more rapid and multiexponential. The overall intensity of the fluorescence decreases, but there is no change in the shape of the steady-state emission spectrum (not shown).

A charge-transfer complex is known to be formed by TNF/TP6EO2M,[42,43] which acts as a quencher of TP6EO2M fluorescence, and the decrease in fluorescence emission intensity and faster fluorescence decay rate as the dopant is added reflect this quenching process.

The time resolved fluorescence decays in doped one-dimensional systems have been modeled by a random walk on a linear chain incorporating traps.[50−54] Traps may be considered as being "deep" if they cause rapid relaxation of the exciton, or "shallow" if the possibility that the exciton might escape is allowed for. The trap may be a chemical impurity (an extrinsic trap such as TNF or oxygen) or a structural defect caused by fluctuations in molecular spacing within the aggregate (an intrinsic trap). Sites at which the nonradiative decay rate is high, such as the ends of the aggregates that are partially exposed to solvent, would have the same effect as intrinsic traps, i.e., to reduce the number density of excitons. For a low concentration ($<10^{-2}$ mole fraction) of randomly distributed deep traps, the long-time exciton decay defined by $t > \tau_h/(\pi^2 x_{trap}^2)$, is described by,[10,18,53,55−57]

$$\frac{n(t)}{n(0)} = x_{trap}\left(\frac{t}{\tau_h}\right)^{1/2} \exp\left[-1.9\left(\frac{\pi^2 x_{trap}^2 t}{\tau_h}\right)^{1/3} - \frac{t}{\tau}\right] \qquad (1)$$

where $n(t)$ and $n(0)$ are the exciton mole fractions at time t and $t = 0$ respectively, τ is the exciton lifetime in the absence of traps, x_{trap} is the trap mole fraction, and τ_h is the exciton hopping time. Since, $n(t)/n(0)=I(t)/I(0)$, where $I(t)$ and $I(0)$ are the fluorescence intensities at time t and $t = 0$, respectively, eq 1 may be rewritten as

$$I(t) = A\sqrt{t}\exp(-Bt^{1/3} - t/\tau) \qquad (2)$$

where $A = x_{trap}/\tau_h^{1/2}$ and $B = 1.9((\pi^2 x_{trap}^2)/(\tau_h))^{1/3}$ and the equation is valid for $t > (1.9/B)^3$.

The time resolved fluorescence data were fitted with this model by iterative reconvolution with an instrument function using in-house software. The quality of the fit was evaluated

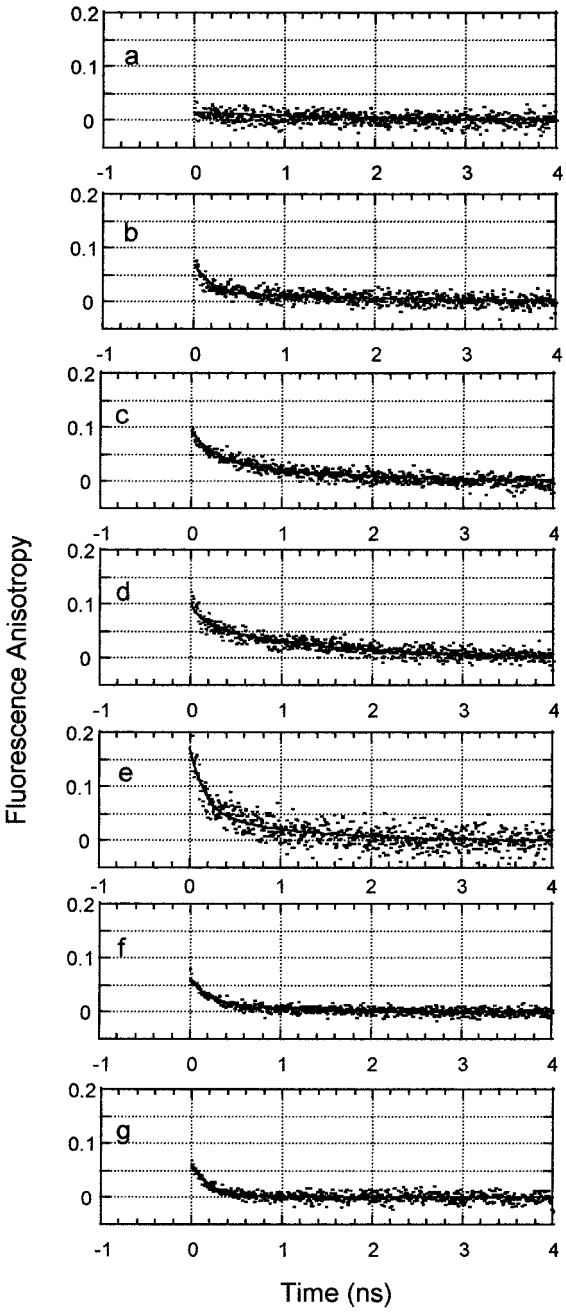

Figure 5. Time resolved fluorescence anisotropy decays of TP6EO2M in D_2O [(a) 10^{-1} M, (b) 10^{-2} M, (c) 10^{-3} M, (d) 10^{-4} M, and (e) 10^{-5}M] and in DCM [(f) 10^{-1} M and (g) 10^{-5} M]. In all cases excitation wavelength was 365 nm and emission wavelength was 389 nm. The fitted curves correspond to a biexponential decay with time constants, τ_1 and τ_2, and initial anisotropy value at $t = 0$ of r_o summarized in Table 3.

by the χ^2 formalism and inspection of the residuals using least-squares analysis. The choice of τ, the value of the exciton lifetime in the absence of traps, which is a constant for the system, had little effect on the results of the fitting for values chosen between the fluorescence and radiative lifetimes, so it was fixed at 25 ns. A summary of the fitting results is given in Table 4.

As the trap concentration is increased the value of B obtained from the fitting increases, as would be expected assuming that the hopping rate is unaffected. However, the values of hopping time ($>10^{-9}$ s^{-1}) are several orders of magnitude greater than the anisotropy data indicate ($<10^{-10}$ s^{-1}). This very poor agreement is due to the high concentration of intrinsic traps in the system, which the fitting to the doped data reveals to be of the order 4×10^{-2} mole fraction (see Table 4), which is outside the limit of validity of the model. (The intrinsic trap concentration can be confirmed by a simple inspection of the raw fluorescence decay data of the doped aggregates. The fluorescence decay of the doped system does not change significantly until the dopant concentration reaches approximately 10^{-2} mole fraction. This indicates that the intrinsic trap concentration within the aggregates is of that order of magnitude since the presence of extrinsic traps will only cause a noticeable change in the fluorescence decay kinetics when their concentration is comparable to the intrinsic trap concentration.) The concentration of intrinsic traps in the isotropic phase of this lyotropic system is an order of magnitude higher than in the case of the thermotropic analogue HAT6.[19] This reflects the absence of well-aligned microdomains that exist in the thermotropic mesophase and the multiplicity of sites which can cause the exciton to relax in the lyotropic system such as the ends of the aggregates and structural defects caused by aggregate flexibility.

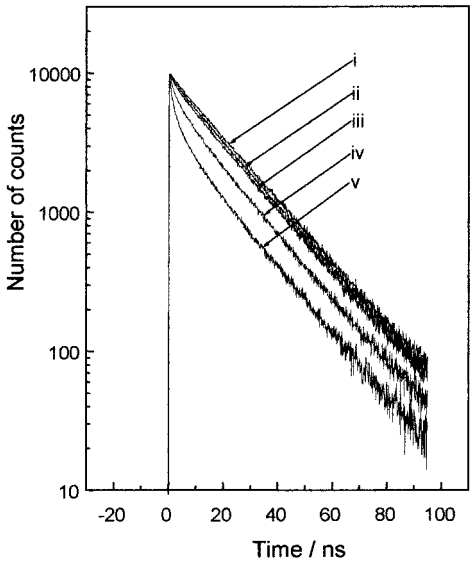

Figure 6. Fluorescence decays of 10^{-2} M TP6EO2M doped with varying amounts of TNF in D_2O: (i) undoped and 2×10^{-3} mole fraction TNF, (ii) 4×10^{-3} mole fraction, (iii) 10^{-2} mole fraction, (iv) 4×10^{-2} mole fraction, (v) 8×10^{-2} mole fraction. Emission wavelength was 389 nm and excitation wavelength was 281 nm in all cases.

TABLE 4: Summary of the Results of Fitting the Time Resolved Fluorescence Decays of 10^{-2} M TP6EO2M in D_2O (Figure 6) Doped with TNF with the 1-D Hopping Model in Eq 2[a]

x_{TNF} (mole fraction)	B ($s^{-1/3}$)	τ_h (ns)	χ^2
0	0.385		1.09
2×10^{-3}	0.396	2.47	1.20
4×10^{-3}	0.410	1.87	1.52

[a] The value of τ, the lifetime of the exciton in the absence of traps, a constant for the system, had little effect on the value of B obtained and was fixed to 25 ns. Quality of fit is indicated by the χ^2 value and evaluated by inspection of the residuals.

Conclusions

The steady state and time resolved phophysical properties of a novel self-assembling lyotropic discotic liquid crystal, 2,3,6,7,10,11-hexa-(1,4,7-trioxaoctyl)-triphenylene (TP6EO2M) have been reported. This system was studied in a part of the phase

diagram which comprises a concentration dependent distribution in size of linear aggregates isolated from each other in isotropic solution, thus providing a potentially true 1-D system for energy migration, and one in which the effect of entry in to the liquid crystalline phases can also be studied for comparison.

The spectral changes in the absorption and steady state and time resolved fluorescence data which accompany changes in TP6EO2M concentration, i.e., aggregate size, have been shown to be due to a property of self-assembly rather than due to a change in the local dielectric constant of chromophores as the solvent is excluded. There is no evidence of excited-state delocalization such as one observes in some conjugated polymers (in this self-assembling system the disc−disc separation is quite large ~4.5 Å), and the evidence suggests only a very weak interaction between neighboring molecules. A model is proposed in which a localized but mobile exciton hops along the columnar aggregates until a trap site or an end of the aggregate is reached, which causes nonradiative relaxation to the ground state.

Time resolved fluorescence depolarization measurements support this picture of a mobile exciton because a rapid initial depolarization is observed in the longer aggregates in which one might expect a slower loss in fluorescence polarization by rotational diffusion if the excited state were stationary. The anisotropy data indicate that the hopping rate is at least 10^{11} s^{-1}.

Doping of the molecular aggregates using trinitrofluorononone (TNF) has revealed that the intrinsic trap concentration in this system (4×10^{-2} mole fraction) is an order of magnitude higher than in the thermotropic analogues. This reflects the absence of well-aligned microdomains and the role of the ends of the aggregates and structural defects caused by aggregate flexibility as sites with high nonradiative relaxation rates. Fitting the doped fluorescence data with a simple 1-D model is unable to yield a value for the hopping rate since the high intrinsic trap concentration places the total trap concentration at the limit of validity for this model.

We have shown that the lyotropic analogue of the much studied HAT-*n* thermotropic liquid crystals demonstrates similar exciton kinetics, but in contrast to the self-organizing thermotropic systems that do not display truly 1-D singlet exciton dynamics, these self-assembling systems have phase structures that comprise individual linear molecular aggregates in solution, effectively isolated from each other, which offer promise for 1-D energy (and charge) conduction. The observation of 1-D energy transport in these systems, reported here for the first time, suggests that lyotropic discotic liquid crystals may be an important class of material for the molecular electronic and photonic devices of the future.

Acknowledgment. The authors thank the EPSRC for financial support.

References and Notes

(1) Boden, N.; Movaghar, B. *Handbook of Liquid Crystals*; Wiley−VCH: New York, 1998; Vol. 2B.

(2) Adam, D.; Schuhmacher, P.; Simmerer, J.; Haussling, L.; Siemensmeyer, K.; Etzbach, K. H.; Ringsdorf, H.; Haarer, D. *Nature* **1994**, *371*, 141.

(3) Schouten, P. G.; Warman, J. M.; de Haas, M. P.; Fox, M. A.; Pan, H.-L. *Nature* **1991**, *353*, 736.

(4) Kemp, M.; Roitbeg, A.; Mijica, V.; Wanta, T.; Ratner, M. *J. Phys. Chem.* **1996**, *100*, 8349.

(5) Hochstrasser, R. M.; Whiteman, J. D. *J. Chem. Phys.* **1972**, *56*, 5945.

(6) Dlott, D. D.; Fayer, M. D.; Wieting, R. D. *J. Chem. Phys.* **1977**, *67*, 3808.

(7) Dlott, D. D.; Fayer, M. D.; Wieting, R. D. *J. Chem. Phys.* **1978**, *69*, 2752.

(8) Auerbach, R. A.; McPherson, G. L. *Phys. Rev. B* **1987**, *33*, 6815.

(9) Knochenmuss, R.; Gudel, H. V. *J. Chem. Phys.* **1987**, *11*, 1104.

(10) Rodrigues, W. J.; Auerbach, R. A.; McPherson, G. L. *J. Chem. Phys.* **1986**, *85*, 6442.

(11) Peterson, K.; Fayer, M. D. *J. Chem. Phys.* **1986**, *85*, 4702.

(12) Webber, S. E.; Swenberg, C. E. *Chem. Phys.* **1980**, *49*, 231.

(13) Markovitsi, D.; Tran-Thi, T.; Briois, V.; Simon, J.; Ohta, K. *J. Am. Chem. Soc.* **1988**, *110*, 2001.

(14) Markovitsi, D.; Lecuyer, I.; Simon, J. *J. Phys. Chem.* **1991**, *95*, 3620.

(15) Markovitsi, D.; Hanack, M.; Vermehren, P. *J. Chem. Soc., Faraday Trans.* **1991**, *87*(3), 455.

(16) Ecoffet, C.; Markovitsi, D.; Millie, P.; Lemaistre, J. *Chem. Phys.* **1993**, *177*, 629.

(17) Markovitsi, D.; Rigaut, F.; Mouallem, M.; Malthete, J. *Chem. Phys. Lett.* **1987**, *135*, 236.

(18) Markovitsi, D.; Lecuyer, I.; Lianos, P.; Malthete, J. *Chem. Soc., Faraday Trans.* **1991**, *87*(11), 1785.

(19) Markovitsi, D.; Germain, A.; Mille, P.; Lecuyer, I.; Gallos, L. K.; Argyrakis, P.; Bengs, H.; Ringsdorf, H. *J. Phys. Chem.* **1995**, *99*, 1005.

(20) Markovitsi, D.; Sigal, H.; Lazaros, K.; Argyrakis, G.; Argyrakis, P. *J. Phys. Chem.* **1996**, *100*, 10999.

(21) Marguet, S.; Markovitsi, D.; Millie, P.; Sigal, H.; Kumar, S. *J. Phys. Chem. B* **1998**, *102*(24), 4697.

(22) Markovitsi, D.; Marguet, S.; Gallos, L. K.; Sigal, H.; Millie, P.; Argyrakis, P.; Ringsdorf, H.; Kumar, S.; *Chem. Phys. Lett.* **1999**, *306*(3−4), 163.

(23) Markovitsi, D.; Marguet, S.; Bondkowski, J.; Kumar, S.; *J. Phys. Chem. B*, **2001**, *105*, 1299.

(24) Boden, N.; Bushby, R. J.; Ferris, L.; Hardy, C.; Sixl, F. *Liq. Cryst.* **1986**, *1*(2), 109.

(25) Boden, N.; Bushby, R. J.; Hardy, C.; Sixl, F. *Chem. Phys. Lett.* **1986**, *123*(5), 359.

(26) Hubbard, J. F., Ph.D. Thesis, University of Leeds, 1997.

(27) Wood, A., Ph.D. Thesis, University of Leeds, 1996.

(28) Eichhorn, H.; Wohrle, D.; Pressner, D. *Liq. Cryst.* **1997**, *22*(5), 643.

(29) Praefke, K.; Singer, D.; Gundogan, B.; Gutbier, K.; Langner, M. *Ber. Bunsen-Ges. Phys. Chem.* **1998**, *98*, 118.

(30) Usol'Tseva, N.; Praefke, K.; Singer, D.; Gundogan, B. *Liq. Cryst.* **1994**, *16*, 601.

(31) Bast, T.; Hentscke, R. *J. Phys. Chem.* **1996**, *100*, 12162.

(32) Edwards, R. G.; Henderson, J. R.; Pinning, R. L. *Mol. Phys.* **1995**, *86*(iv), 567.

(33) Attard, P. *Mol. Phys.* **1996**, *89*, 691.

(34) Taylor, M. P.; Herzfeld, J. *Phys. Rev. A* **1991**, *43*, 1892.

(35) Cotter, M. A.; Wacker, D. C. *Phys. Rev. A* **1978**, *18*, 2669.

(36) Hartshorne, N. H.; Woodard, G. D. *Mol. Cryst. Liq. Cryst.* **1973**, *23*, 343.

(37) Hentschke, R.; Edwards, P. J. B.; Boden, N.; Bushby, R. J. *Macromol. Symp.* **1994**, *81*, 361.

(38) Van der Schoot, P.; Cates, M. E. *Europhys. Lett.* **1994**, *25*, 515.

(39) Israelachvili, J. *Intermolecular and Surface Forces*; Academic Press: San Diego, 1991; Vol. 2, pp 341−394, and references therein.

(40) Henderson, J. R. *Phys. Rev. E* **1996**, *77*(11), 2316.

(41) Hughes, R.; Smith, D. A.; Bushby R.; Movaghar, B.; Boden, N. *Mol. Cryst. Liq. Cryst.* **1999**, *332*, 547.

(42) Ebert, M.; Frick, G.; Baehr, C. H.; Wendorff, J. H.; Wustefeld, R.; Ringsdorf, H. *Liq. Cryst.* **1992**, *11*, 293.

(43) Bengs, H.; Ebert, M.; Karthaus, O.; Ringsdorf, H.; Wustefeld, R. *Liq. Cryst.* **1990**, *2*, 141.

(44) Boden, N.; Bushby, R. J.; Clements, J.; Luo R. *J. Mater. Chem.* **1995**, *5*(10), 1741.

(45) Hughes, R. E.; Ph.D. Thesis, University of Leeds, 2000.

(46) Bassler, H.; Brandl, V.; Deussen, M.; Gobel, E. O.; Kersting, R.; Kurz, H.; Lemmer, U.; Mahrt, R. F.; Ochse, A. *Pure Appl. Chem.* **1995**, *37*(3), 377.

(47) Baunsgaard, D.; Larsen, M.; Harrit, N.; Frederiksen, J.; Wilbrandt, R.; Stapelfeldt, H. *J. Chem. Soc., Faraday Trans.* **1997**, *93*(10), 1893.

(48) Biasutti, M. A.; De Feyter, S.; De Backer, S.; Dutt, G. B.; De Schryver, F. C.; Ameloot, M.; Schlichting, P.; Müllen, K. *Chem. Phys. Lett.* **1996**, *248*, 13.

(49) Forster, Th. *Discuss Faraday Soc., Ann. Phys.* **1948**, *2*, 55.

(50) Montroll, E. W.; Weiss, G. H. *J. Math. Phys*. **1965**, *6*, 167.

(51) Zumofen, G.; Blumen, A. *Chem. Phys. Lett*. **1982**, *88*, 63.

(52) Movaghar, B.; Pohlmann, B.; Wurz, D. *Phys. Rev. A* **1984**, *29*, 1568.

(53) Movaghar, B.; Sauer, G.; Wurz, D. *Solid State Commun*. **1981**, *39*, 1179. Movaghar, B.; Sauer, G.; Wurz, D. *J. Stat. Phys*. **1982**, *27*, 473.

(54) Alexander, S.; Bernasconi, J.; Schneider, W.; Orbac, R. *Rev. Mod. Phys*. **1981**, *53*, 175, and references therein.

(55) Blumen, A.; Klafter, J.; Zumofen, G. *Optical spectroscopy of glasses*, 1st ed.; Kluwer Academic: Dordrecht, 1986; pp 199−265.

(56) Opniko, A. I.; Malysheva, L. I.; Zozulenko, I. V. *Chem. Phys*. **1988**, *121*.

(57) Redner, S.; Kang, K. *Phys. Rev. Lett*. **1983**, *51*, 1729.